文章编号:0253-9985(2023)04-0910-13 doi:10.11743/ogg20230409

陆相页岩游离油定量表征及其影响因素
——以苏北盆地高邮凹陷古近系阜宁组二段为例

刘 天[1,2],刘小平[1,2],刘启东[3],段宏亮[3],刘世丽[3],孙 彪[1,2],化祖献[1,2]

[1. 中国石油大学(北京)油气资源与工程全国重点实验室,北京 102249;2. 中国石油大学(北京)地球科学学院,北京 102249;3. 中国石化 江苏油田分公司 勘探开发研究院,江苏 扬州 225009]

摘要:为准确、定量评价陆相页岩游离油量及其影响因素,选取了苏北盆地高邮凹陷古近系阜宁组二段陆相页岩样品,利用全岩X射线衍射分析、有机碳测定、多温阶热释烃、高压压汞、有机质抽提和二维核磁共振等实验技术手段,分析了页岩样品矿物成分、生烃品质、孔隙结构和含油性等特征。结果表明,页岩富含石英、长石、方解石、白云石以及黏土矿物等成分;总有机碳含量(*TOC*)为0.61%~3.70%,镜质体反射率(R_o)为0.70%~0.72%,处于成熟阶段;储集空间主要为晶间孔、粒间孔和有机孔。二维核磁共振可以有效表征页岩游离油赋存状态。抽提分离出页岩储层内可动用的游离态轻、重烃类化合物和可溶有机质,对抽提前、后页岩样品进行二维核磁共振谱图分析,将谱图划分出轻质油和类固体有机质等区域。抽提后类固体有机质含量和*TOC*有良好相关关系,抽提前核磁轻质烃含量和核磁轻质烃抽提差都与热解游离油量有较好线性关系。游离油量随着长英质矿物含量增加先增大后减小,与*TOC*含量整体上为正相关关系;Ⅰ型和$Ⅱ_1$型干酪根有机质页岩游离油量较其他类型高;适中的成熟度演化使干酪根生成烃类轻组分增多、可动性增强,游离油量增多。高孔隙度、高比孔体积及高孔喉半径均值的页岩储层有利于游离油富集。

关键词:游离油量;核磁共振;阜宁组;陆相页岩;高邮凹陷;苏北盆地
中图分类号:TE122.1 **文献标识码:**A

Quantitative characterization and influencing factors of free oil content in lacustrine shale: A case study of Funing Formation in the Gaoyou Sag, Subei Basin

LIU Tian[1,2], LIU Xiaoping[1,2], LIU Qidong[3], DUAN Hongliang[3], LI Shili[3], SUN Biao[1,2], HUA ZuXian[1,2]

[1. *National Key Laboratory of Petroleum Resources and Engineering*, *China University of Petroleum (Beijing)*, *Beijing* 102249, *China*; 2. *College of Geosciences*, *China University of Petroleum (Beijing)*, *Beijing* 102249, *China*; 3. *Research Institute of Exploration and Development*, *SINOPEC Jiangsu Oilfield Company*, *Yangzhou*, *Jiangsu* 225009, *China*]

Abstract: The lacustrine shale samples were selected from the second member of the Funing Formation in Gaoyou Sag, Subei Basin, to precisely and quantitatively evaluate the free oil content and its controlling factors of lacustrine shale. The mineral composition, hydrocarbon generation capacity, pore structure, oil-bearing properties, and other characteristics of the samples were analyzed using X-ray diffraction tests, *TOC* content measurement, multistep rock-eval pyrolysis, high pressure mercury injection, organic matter extraction and 2D NMR. The results show that the shale is rich in quartz, feldspar, calcite, dolomite, clay, and other minerals. The *TOC* is between 0.61 % and 3.70 %. The R_o is between 0.70 % and 0.72 %, indicating the source rocks being in the mature stage. The reservoir space is mainly composed of intergranular and organic pores. Two-dimensional NMR, which can efficiently detect and characterize the occurrence of free oil, was employed to help extracting free light and heavy hydrocarbons as well as soluble organic matter from the samples, and performing spectra analysis before and after the extraction, on which light oil zone, solid organic matter zone, hydroxyl compound zone, and water zone were identified. Post-extraction solid organic matter content was found to have a good correlation with *TOC*. Pre-extraction NMR-based light hydrocarbon

收稿日期:2023-02-23;**修回日期:**2023-06-17。
第一作者简介:刘天(1997—),男,博士研究生,非常规油气地质。**E-mail:** 13804341768@163.com。
通信作者简介:刘小平(1971—),男,教授、博士生导师,石油地质。**E-mail:** liuxiaoping@cup.edu.cn。
基金项目:国家自然科学基金项目(42072150)。

content and NMR-based differential light hydrocarbon content between pre-extraction and post-extraction show a relatively strong linear connection with pyrolysis free oil content. The free oil content rises initially and then fall as the felsic mineral content rises, and it is positively correlated with *TOC* as a whole. The free oil contents in type Ⅰ and $Ⅱ_1$ kerogen source rocks are higher than those of other kinds. The right degree of thermal evolution of source rocks increases the ratio of light hydrocarbons and mobility of kerogen-generated hydrocarbons, as well as free oil content. Shale reservoirs with high porosity, specific pore volume, and median value of pore throat radius are conducive to free oil enrichment.

Key words: free oil content, nuclear magnetic resonance, Funing Formation, lacustrine shale, Gaoyou Sag, Subei Basin

引用格式:刘天,刘小平,孙彪,等. 陆相页岩游离油定量表征及其影响因素——以苏北盆地高邮凹陷古近系阜宁组二段为例[J]. 石油与天然气地质,2023,44(4):910-922. DOI:10. 11743/ogg20230409.

LIU Tian, LIU Xiaoping, SUN Biao, et al. Quantitative characterization and influencing factors of free oil content in lacustrine shale[J]. Oil & Gas Geology,2023,44(4):910-922. DOI:10. 11743/ogg20230409.

常规油气产量难以满足日渐增长的油气需求,各国油气勘探开发目标都在从常规油气转向非常规油气新领域。随着近年对新油气领域的不断探索,非常规油气资源的地位在当前能源需求中不断上升,美国页岩油气革命改变了世界能源格局,拓展了油气资源的勘探开发领域。北美海相页岩沉积主要形成于缺氧、低能的海相沉积环境,页岩层系分布面积大,盆地构造稳定性好,优质烃源岩大面积稳定发育,岩相类型相对单一,页岩油油质轻、黏度低[1-4]。中国页岩油勘探开发起步较晚,随着油气地质理论的突破创新和工程技术的进步,鄂尔多斯盆地、准噶尔盆地、三塘湖盆地、松辽盆地、渤海湾盆地、苏北盆地、四川盆地等的陆相页岩油勘探开发均取得了重大突破[5-11]。中国陆相页岩主要形成于半深水—深水湖相沉积环境,页岩层系分布面积较小、岩相类型多样,盆地构造活动性强,页岩油以重质组分为主,黏度高、气油比低[12-13]。中国陆相页岩与北美海相页岩相比地质条件更为复杂,主要在3个方面亟待研究:①陆相页岩沉积相变快,页岩油源储非均质性强;②陆相未熟-低熟富有机质页岩分布广,页岩油黏度高、可流动性较差;③陆相页岩储层矿物成分和孔隙结构类型复杂多变,原油流动机理和有效动用条件不明。

页岩油在纳米孔隙内主要以吸附态和游离态两种形态存在,游离态油赋存于微裂缝、层间隙以及孔隙中,不受分子间相互作用力束缚可以流动;吸附态油吸附于岩石矿物表面或者干酪根刚性大分子骨架内外表面,没有流动性,以高密度的"固体"形式存在[14-15]。目前技术件下,游离态油是产出页岩油中的主要构成部分。页岩游离油量表征方法主要有热解S_1法[15-16]、含油饱和度法[17]、荧光定量法[18-19]、溶剂萃取法[20]、核磁法[21-23]及分子模拟法[24-25]等手段,热解S_1法简单快捷,能实现不同赋存状态页岩油分离及定量表征,然而因存在轻烃散失而需要校正结果;溶剂抽提法分析过程复杂繁琐,同样存在轻烃散失,溶剂、粒径以及抽提方式的改变也会引起实验结果的变化;核磁共振离心法实验无损快速,但由于矿物、储层致密等因素导致驱替不充分,无法有效充分表征游离油量;分子模拟法可有效模拟游离油微观赋存特征,但模拟条件单一,难以有效复现游离油复杂赋存特征。页岩含油性非均质性极强,游离油量受岩相、矿物组分、有机质(丰度、类型和成熟度)及润湿性、孔隙结构、原油物理化学性质(密度、黏度、含蜡量、族组分、气油比等)、温度与压力等诸多因素影响,已有学者对页岩游离油赋存及其影响因素开展了一定研究,但相关的认识尚未统一[26-27]。

苏北盆地高邮凹陷古近系阜宁组二段(阜二段)页岩油取得重大突破,部署井成功放喷投产,然而对页岩游离油缺乏精细表征等相关研究,页岩游离油分布非均质性强、富集高产因素认识不清。本文基于全岩衍射分析、有机碳测定、常规热解及高压压汞等实验,利用多温阶热解、二维核磁共振及有机质抽提等手段定量表征了页岩游离油量,对不同赋存状态页岩油进行了定量分析,明确了阜二段页岩矿物组分、有机质及储层对页岩游离油量的影响,系统探讨了中低成熟度页岩游离油影响因素,为苏北盆地高邮凹陷页岩油勘探选区和目标评价奠定基础,对于深化陆相页岩游离油富集规律认识具有一定指导意义。

1　地质概况

苏北盆地面积3. 6×10^4 km^2,位于中国东部江苏省和安徽省之间。苏北盆地受造山带及断裂带控制,是形成于晚白垩世的一个裂谷盆地。自白垩世以来,苏北盆地经历了仪征、吴堡、真武和三垛4次大构造运动。苏北盆地构造演化可分为张性断裂阶段、后期断裂阶段及拗陷阶段。苏北盆地构造格局复杂,整体表现为

"两坳一隆"。两个坳陷中分布多个小型凹陷或凸起，中间受建湖隆起相隔。高邮凹陷为苏南隆起、柘垛及吴堡低凸起围绕，东接白驹凹陷[28]。高邮凹陷围绕其沉降中心，由南向北发育深凹带、断阶带及斜坡带，取样井X1井是在苏北盆地高邮凹陷花庄地区阜二段部署的页岩油井。阜宁组位于下部断-坳陷期构造层，广泛分布于苏北盆地各凹陷（图1）。按照沉积环境和岩性组合特征阜宁组自下而上可划分为阜一段至阜四段[29]。高邮凹陷阜二段总厚度可达300 m以上，沉积环境为半深湖-深湖，根据岩性将阜二段分为5个亚段。

2 样品和实验

2.1 样品

为了系统进行苏北盆地高邮凹陷阜二段游离油定量表征及其影响因素研究，采集了苏北盆地高邮凹陷X1井阜二段页岩样品，岩性主要为页岩（图1）。样品分析包括X射线衍射定量30个样品、高压压汞实验11个样品、有机质抽提及二维核磁共振5个样品、常规热解、冷冻热解和有机碳定量分析30个样品。

2.2 实验

页岩样品自地下采集至开展测试分析前普遍存在3个阶段轻烃散失：①页岩离开地下到达地面后，温-压条件改变致使气态烃膨胀快速散失；②在没有包裹封闭的条件下，入库保存的页岩样品轻烃组分发生缓慢散失；③页岩样品因分析测试前的样品加工或粉碎破坏原始储集条件而造成烃类组分散失[30]。本次研究通过两组页岩样品开展轻烃恢复校正：一组页岩样品在密闭取心、液氮保存条件下进行冷冻碎样热解实验；另一组页岩样品放置一个月后进行热解实验。两组页岩样品在采集、放置及实验处理中所测得累积差值即为轻烃散失量。

多温阶热释烃分析使用Rock-Eval 6仪器进行，共计30个样品。起始温度200 ℃并恒温1 min得到S_{1-1}，为热挥发轻质组分含量。温度段200～350 ℃得到S_{1-2}，为中-高分子量组分含量。温度段350～450 ℃时得到S_{2-1}，为吸附态的胶质、沥青质和稠油组分含量。温度段450～600 ℃得到S_{2-2}，为干酪根热降解生成的组分含量。其中S_{1-1}反映的是实际游离油量，$S_{1-1}+S_{1-2}$反映了最大游离油量，S_{1-2}反映的是吸附油量[16]。

二维核磁共振实验使用美国岩心公司MRCore-040V型23 MHz核磁共振仪器，定量检测常规处理下页岩样品内含^{1}H化合物的纵向弛豫时间（T_1）和横向弛豫时间（T_2），共计5个样品。有机质抽提实验利用DCM溶剂通过索氏萃取法对样品内可溶于溶剂的物质进行抽提，萃取在70 ℃下进行48 h以量化页岩样品中的滞留油。提取实验后，再次进行二维核磁共振实验。

高压压汞使用安东帕康塔PoreMaster 60压汞仪，在25 ℃环境下对有机质抽提后圆柱状页岩样品施加压力0.001～400 MPa，共计11个样品。对汞施加的压力大于或等于孔隙喉道的毛管压力时，汞就克服毛管

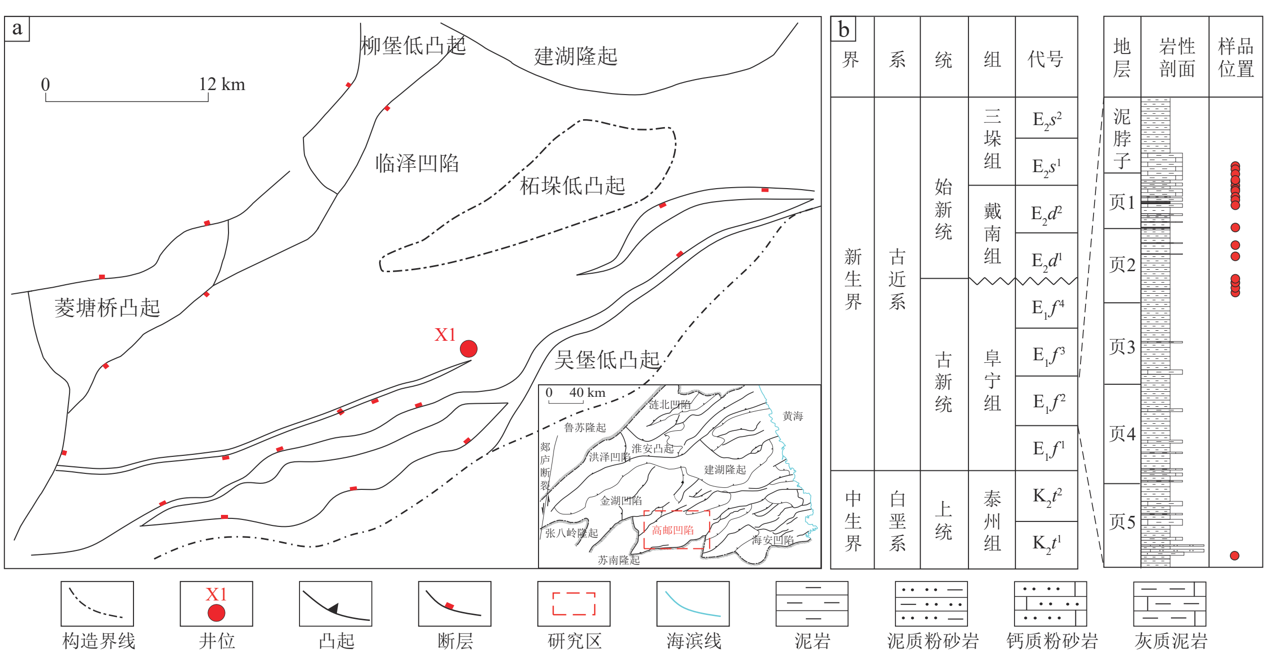

图1 苏北盆地高邮凹陷区域构造位置（a）和地层综合柱状图（b）

Fig. 1 Structure location (a) and stratigraphic column (b) of Gaoyou Sag, Subei Basin

阻力进入孔隙,根据进汞的孔隙体积分数和对应压力,可以得到毛管压力与岩样含汞饱和度的关系,根据测得的毛管压力曲线换算孔隙大小及孔径分布。

3　实验结果

3.1　岩石学特征

高邮凹陷阜二段页岩样品由多种矿物组成。矿物组分以黏土矿物、石英、白云石、长石和方解石为主,矿物含量范围分别为9.4 %～56.2 %,9.3 %～41.4 %,1.0 %～68.0 %,0.9 %～27.9 %和0.4 %～41.3 %,矿物组分平均含量分别为32.7 %,26.1 %,20.3 %,11.7 %和9.2 %。页岩矿物可分为长英质(石英和长石)、黏土矿物和碳酸盐矿物(方解石、白云石和铁白云石)[31],平均含量分别为36.3 %,28.2 %和31.3 %(图2;表1)。

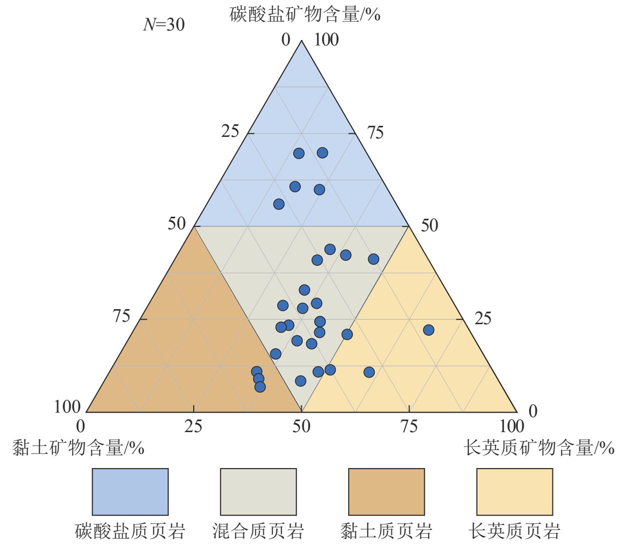

图2　高邮凹陷X1井阜二段页岩矿物组分含量三端元图

Fig. 2　Ternary diagram showing mineral components of E_1f^2 shale of Well X1 in Gaoyou Sag

表1　高邮凹陷X1井阜二段页岩矿物组分含量

Table 1　Mineral components of E_1f^2 shale of Well X1 in Gaoyou Sag

样品编号	岩性	深度/m	矿物成分含量/%				
			黏土矿物	石英	长石	方解石	白云石
S-1	黏土质页岩	3 119.35	54.89	25.05	9.15	7.07	3.85
S-2	长英质页岩	3 120.49	9.39	41.41	27.07	12.32	9.80
S-3	混合质页岩	3 121.92	40.66	33.78	14.68	5.03	5.85
S-4	混合质页岩	3 123.95	41.21	23.74	11.61	10.46	12.97
S-5	混合质页岩	3 128.17	33.47	30.47	11.71	0.41	23.94
S-6	混合质页岩	3 129.82	35.03	25.28	18.24	18.13	3.32
S-7	混合质页岩	3130.61	48.09	27.61	8.58	7.14	8.58
S-8	碳酸盐质页岩	3 131.00	21.13	14.46	3.74	18.60	42.06
S-9	长英质页岩	3 132.90	28.90	34.69	25.66	0.71	10.04
S-10	混合质页岩	3 133.47	32.86	26.16	8.11	1.84	31.03
S-11	长英质页岩	3 136.02	37.58	23.15	27.86	9.02	2.40
S-12	混合质页岩	3 143.99	31.81	29.42	9.45	9.55	19.76
S-13	混合质页岩	3 149.35	28.87	34.80	15.37	0.99	19.98
S-14	碳酸盐质页岩	3 151.69	15.87	16.18	8.09	16.29	43.57
S-15	混合质页岩	3 161.54	25.84	20.56	12.70	5.96	34.94
S-16	混合质页岩	3 161.87	39.90	22.60	8.77	9.98	18.75
S-17	碳酸盐质页岩	3 162.41	15.79	9.34	5.26	11.60	58.00
S-18	混合质页岩	3 164.93	12.64	28.74	17.45	1.46	39.71
S-19	混合质页岩	3 166.93	21.45	21.23	13.53	28.05	15.73
S-20	混合质页岩	3 357.24	43.27	23.27	10.61	15.82	7.04
S-21	混合质页岩	3 128.47	35.71	25.94	10.38	16.38	11.60
S-22	混合质页岩	3 119.12	18.57	35.12	4.04	41.27	1.01
S-23	混合质页岩	3 114.42	41.37	30.92	8.48	5.17	14.06
S-24	混合质页岩	3 125.07	45.95	32.02	13.62	1.56	6.86
S-25	碳酸盐质页岩	3 128.84	10.20	19.09	0.91	1.82	67.98
S-26	混合质页岩	3 127.68	33.47	30.47	11.71	0.41	23.94
S-27	碳酸盐质页岩	3 129.11	27.23	13.26	3.54	5.36	50.61
S-28	混合质页岩	3 131.49	38.38	32.04	11.16	7.78	10.64
S-29	黏土质页岩	3 124.39	55.39	27.02	8.59	4.29	4.71
S-30	黏土质页岩	3 124.79	56.15	26.68	10.34	1.96	4.86

3.2 有机地化特征

有机质丰度代表着生油岩中有机质的富集程度，决定了生油岩的生烃潜力。TOC是单位质量岩石中有机碳的质量分数；生烃潜量(S_1+S_2)指岩石热解所获得游离烃与干酪根热解烃含量的总和，二者是评价页岩有机质丰富度的重要指标。参照陆相烃源岩有机质评价的行业标准[32]，烃源岩主要为中-好烃源岩(图3a)。

有机质类型决定了有机质生烃能力和生成的烃类产物特征，最高热解峰温(T_{max})和氢指数(HI)之间的关系通常用于有机质类型评估，有机质类型主要为$Ⅱ_1$型，较少Ⅰ型和$Ⅱ_2$型(图3b)。页岩R_o为0.70 %~0.72 %，纵向变化小，处于成熟阶段(表2)。

3.3 储集特征

研究区储集空间发育多种类型，页岩以矿物基质孔为主，包括矿物粒间孔、晶间孔和溶蚀孔，也可见纳米-微米级有机质孔(图4)。阜二段页岩的进汞曲线较为相似，整体呈现两段式特征，在突破排驱压力后，进汞量随着进汞压力的增加而迅速增加。样品S-11和S-5退汞效率较高，孔喉的连通性好、孔喉差异小，比孔体积分别为0.047 cm^3/g和0.045 cm^3/g(图5；表3)。

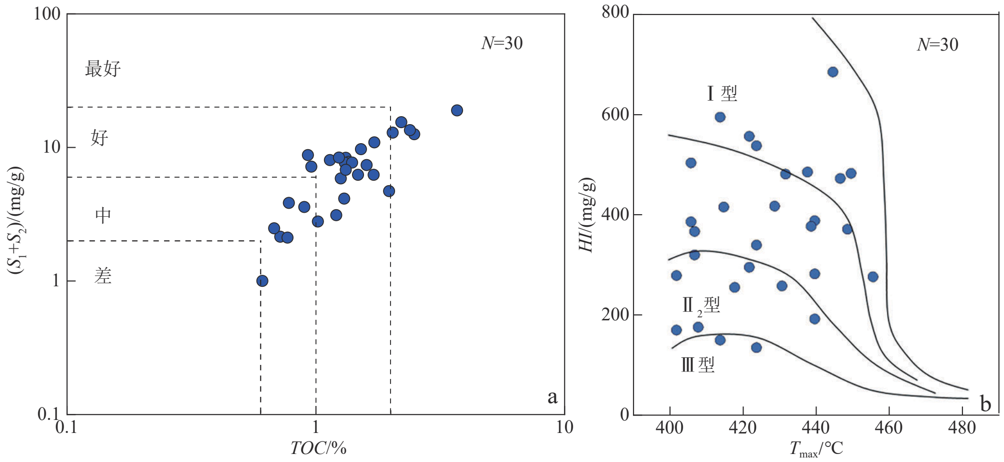

图3 高邮凹陷X1井阜二段烃源岩评价

Fig.3 Evaluation map of E_1f^2 source rocks of Well X1 in Gaoyou Sag

a. TOC与S_1+S_2关系散点图；b. T_{max}-HI交汇图

表2 高邮凹陷X1井阜二段页岩地球化学特征

Table 2 Geochemical characteristics of E_1f^2 shale of Well X1 in Gaoyou Sag

样品编号	TOC/%	S_1/(mg/g)	S_2/(mg/g)	T_{max}/℃	R_o/%	样品编号	TOC/%	S_1/(mg/g)	S_2/(mg/g)	T_{max}/℃	R_o/%
S-1	1.30	0.65	3.26	418	0.705	S-16	1.14	0.74	5.36	447	—
S-2	0.61	0.19	0.45	422	—	S-17	0.90	0.71	2.50	440	—
S-3	1.21	0.60	1.75	414	0.713	S-18	1.24	1.21	5.98	438	—
S-4	0.93	1.32	6.36	445	0.702	S-19	1.52	1.44	7.29	450	0.715
S-5	1.32	0.96	6.61	406	—	S-20	0.68	0.35	1.85	456	0.713
S-6	1.72	0.83	7.09	415	—	S-21	3.70	2.43	14.24	440	—
S-7	1.60	1.01	5.37	424	—	S-22	2.49	1.19	9.30	439	—
S-8	0.78	1.22	2.27	422	—	S-23	2.21	1.68	13.10	414	0.714
S-9	0.72	0.43	1.23	408	0.713	S-24	1.40	1.11	5.08	407	—
S-10	0.77	0.43	1.27	402	—	S-25	2.39	0.68	11.43	432	0.720
S-11	1.36	0.97	5.00	449	0.712	S-26	1.32	0.96	5.05	406	—
S-12	1.31	1.28	5.42	429	0.708	S-27	2.04	1.08	10.92	424	—
S-13	1.26	1.08	3.20	431	—	S-28	0.96	1.02	5.32	422	—
S-14	1.02	0.80	1.32	424	0.706	S-29	1.71	0.62	4.69	402	—
S-15	1.97	0.63	3.69	440	0.705	S-30	1.48	0.77	4.68	407	—

注："—"表示未测得数据。

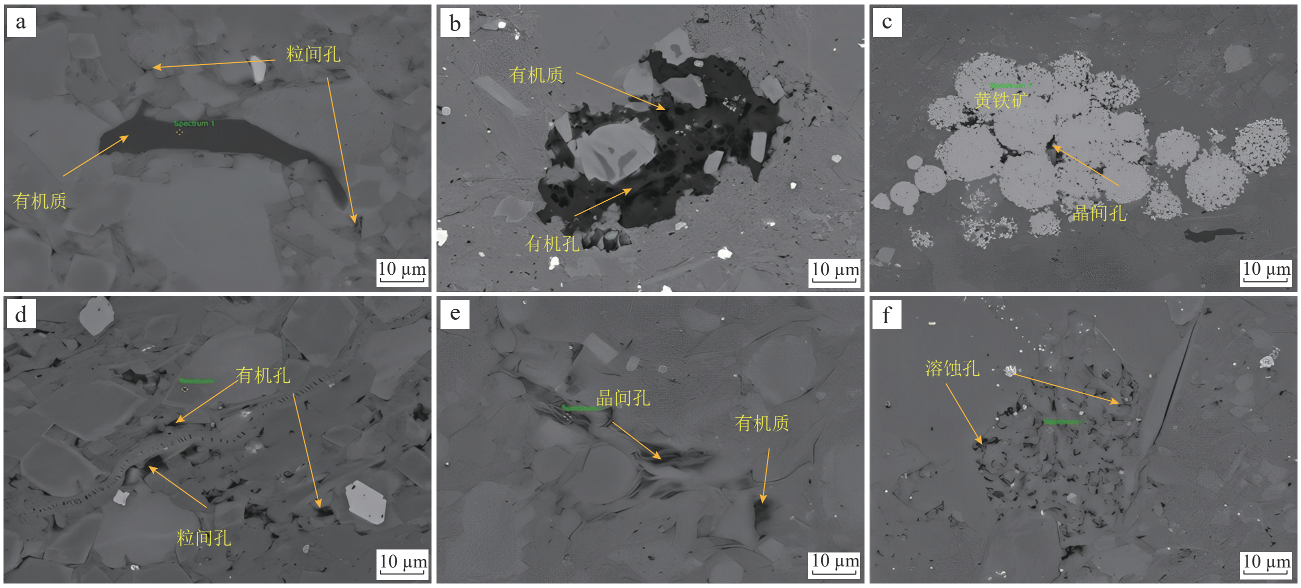

图4　高邮凹陷X1井阜二段页岩孔隙发育特征扫描电镜照片

Fig. 4　Pore characteristics of E_1f^2 shale of Well X1 in Gaoyou Sag

a. 埋深3 118.29 m,页2亚段,可见粒间孔及少量黏土矿物晶间孔;b. 埋深3 143.56 m,页3亚段,蜂窝状有机质孔发育;c. 埋深3 116.45 m,页2亚段,草莓状黄铁矿呈团块状,晶间孔发育;d. 埋深3 134.86 m,页2亚段,有机质、矿物粒间孔发育;e. 埋深3 116.45 m,页2亚段,有机质和黏土矿物共生,黏土矿物晶间孔发育;f. 埋深3 116.45 m,页2亚段,颗粒溶蚀孔隙

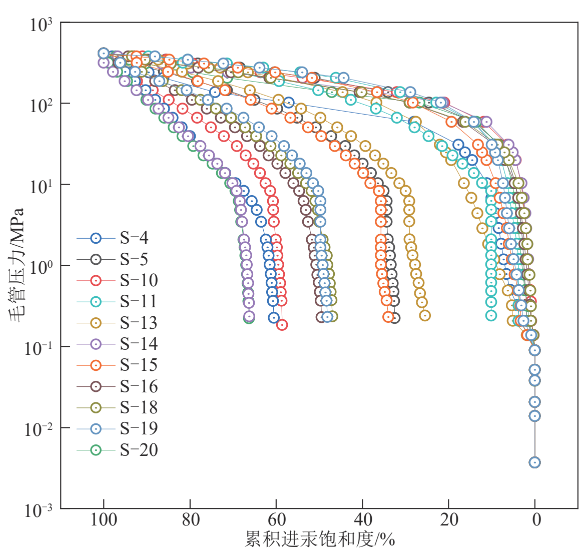

图5　高邮凹陷X1井阜二段页岩高压压汞曲线

Fig. 5　The mercury intrusion curves of E_1f^2 shale at Well X1 in Gaoyou Sag

3.4　含油性特征

对密闭低温保存冷冻处理和常温放置保存常规处理的两组页岩样品分别热解,对比得到轻烃恢复系数,结合多温阶热释烃分析得到校正后游离油量。页岩轻烃散失量为0.23~3.00 mg/g,平均1.02 mg/g;轻烃恢复系数($K_{恢复}$)为1.29~4.61,平均2.15;页岩热解游离油量为1.17~7.41 mg/g,平均为3.81 mg/g(表4;图6)。

对页岩中可动用游离态烃类化合物(轻、重烃类化合物)和可溶有机质进行抽提,抽提后二维谱图中各信号强度减小、总氢含量降低,各区域信号强度有明显减弱(图7)。根据前人研究[33-34],以样品S-11为例,基于T_1/T_2比值和T_2值将谱图划分了4个区域:①区域为类固体有机质信号区,包括干酪根、固体沥青和重质油等;②区域为轻质油,具有较好的可动性;③区域为赋存于页岩孔隙的游离或吸附水;④区域为矿物表面的羟基、结合水或结构水(图7)。

表3　高邮凹陷X1井阜二段页岩储层特征

Table 3　Reservoir characteristics of E_1f^2 shale of Well X1 in Gaoyou Sag

样品编号	孔隙度/%	比孔体积/(cm^3/g)	孔喉半径均值/nm
S-4	7.44	0.036	14.68
S-5	8.24	0.047	15.52
S-10	8.09	0.042	15.43
S-11	9.20	0.045	15.88
S-13	9.03	0.036	16.88
S-14	4.43	0.023	14.47
S-15	7.26	0.045	16.33
S-16	7.64	0.037	15.37
S-18	7.34	0.038	15.43
S-19	5.87	0.029	14.81
S-20	5.57	0.024	14.47

表4 高邮凹陷X1井阜二段页岩含油性参数

Table 4 Oil-bearing parameters of E_1f^2 shale at Well X1 in Gaoyou Sag

样品编号	$K_{恢复}$	含油量/(mg/g)					样品编号	$K_{恢复}$	含油量/(mg/g)				
		$S_{1冷冻}$	S_{1-1}	S_{1-2}	S_{2-1}	游离油量			$S_{1冷冻}$	S_{1-1}	S_{1-2}	S_{2-1}	游离油量
S-1	1.35	0.88	0.41	1.13	2.71	1.77	S-16	3.61	2.67	0.93	2.79	2.04	5.65
S-2	2.89	0.55	0.18	0.81	1.29	1.35	S-17	1.52	1.08	0.29	1.26	1.27	1.92
S-3	2.27	1.36	0.54	1.53	2.03	2.83	S-18	1.98	2.39	0.66	2.51	1.72	4.35
S-4	1.83	2.41	0.54	1.88	1.92	3.51	S-19	1.66	2.39	0.51	3.24	1.29	4.70
S-5	1.81	1.74	0.66	2.05	1.51	3.49	S-20	1.80	0.63	0.21	0.69	2.3	1.17
S-6	4.61	3.83	0.93	3.26	2.53	7.19	S-21	1.91	4.64	1.18	4.02	1.28	7.41
S-7	2.00	2.00	0.94	1.98	2.60	3.92	S-22	2.71	3.23	0.73	3.02	1.72	5.79
S-8	1.29	1.57	0.47	1.94	1.40	2.76	S-23	1.40	2.35	0.60	3.24	3.49	4.51
S-9	2.12	0.91	0.18	0.98	1.28	1.64	S-24	2.36	2.62	0.53	2.29	2.55	4.33
S-10	1.95	0.84	0.30	1.05	1.96	1.76	S-25	2.97	2.02	0.71	2.20	0.95	4.25
S-11	2.87	2.78	0.42	2.36	1.76	4.59	S-26	1.81	1.74	0.66	2.05	2.29	3.49
S-12	1.74	2.23	0.80	2.93	1.41	4.68	S-27	1.81	1.95	0.57	1.98	2.06	3.42
S-13	2.45	2.65	1.00	2.64	2.37	5.21	S-28	1.82	1.86	0.72	1.80	1.89	3.36
S-14	1.84	1.47	0.49	1.91	1.26	3.07	S-29	2.47	1.53	0.79	1.54	2.73	3.24
S-15	1.62	1.02	0.87	4.49	0.66	5.75	S-30	2.01	1.55	0.58	1.85	3.56	3.21

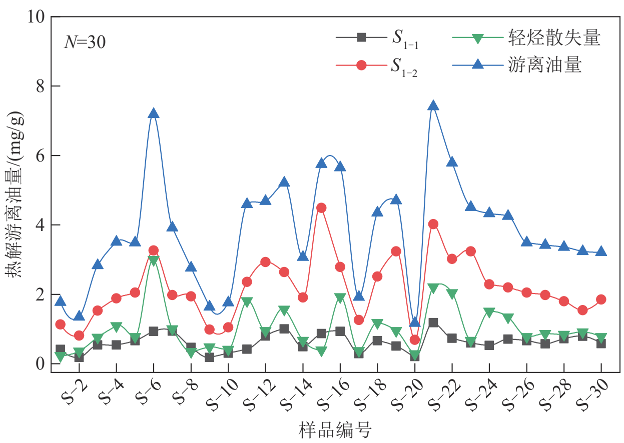

图6 高邮凹陷X1井阜二段页岩热解游离油量

Fig. 6 Free oil contents of E_1f^2 shale at Well X1 in Gaoyou Sag through pyrolysis

根据谱图划分，统计各区间信号强度及总信号占比(表5)，乘以页岩所测得^{1}H化合物总量得到不同相态化合物的绝对量(表6)。抽提前页岩样品类固体有机质含量为2.04～7.00 μL/g，轻质烃含量0.62～1.80 μL/g；抽提后页岩样品类固体有机质含量为0.72～3.77 μL/g，轻质烃含量0.56～1.33 μL/g。

4 讨论

4.1 游离油量定量表征

图7中谱图②区代表页岩中流动性较高轻质烃类流体的信号区间，抽提前核磁轻质烃和热解游离油

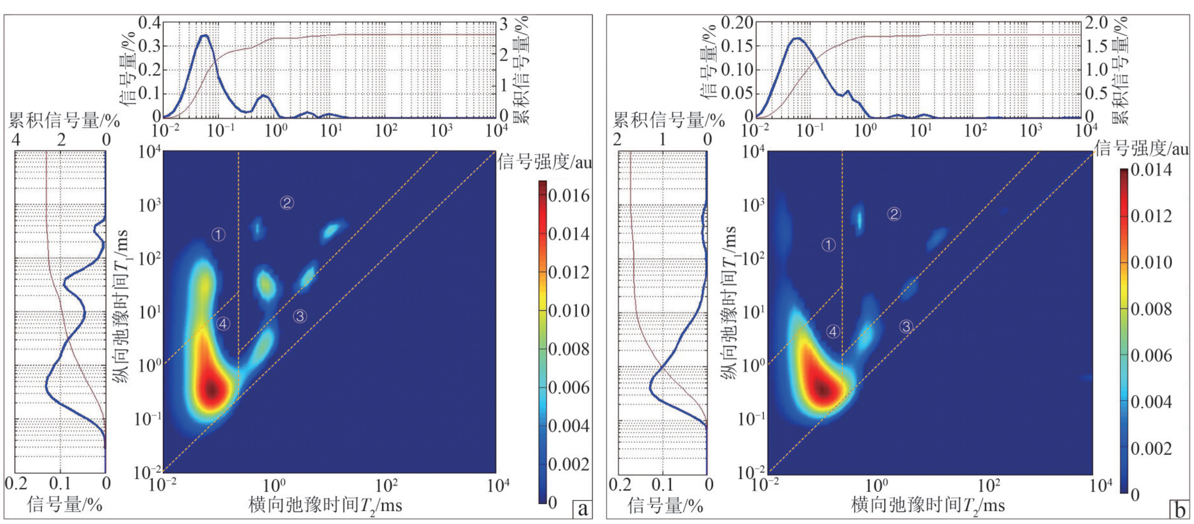

图7 高邮凹陷X1井阜二段页岩样品S-11抽提前(a)、后(b)二维核磁共振谱图

Fig. 7 2D NMR spectra pre-extraction (a) and post-extraction (b) of S-11 from E_1f^2 shale of Well X1 in Gaoyou Sag

(①—④为信号区间。①区域为类固体有机质信号区，包括干酪根、固体沥青和重质油等；②区域为轻质油，具有较好的可动性；③区域为赋存于页岩孔隙的游离或吸附水；④区域为矿物表面的羟基、结合水或结构水。)

量有良好相关关系(图 8a)。有机质抽提对页岩类固体有机质中重质组分、可溶有机质和轻质组分进行了提取(图 8b),核磁轻质烃抽提差和游离油量、抽提后类固体有机质与 *TOC* 有良好的线性关系(图 8c,d),说明抽提后的残留①代表了抽提后残留以吸附态存在的烃类流体化合物和不溶类固体有机质;残留②区间信号代表束缚于孔隙的轻质烃类化合物,在此次的抽提条件下这些有机组分未能实现动用。综上,有机

表 5　高邮凹陷 X1 井阜二段页岩二维核磁抽提信号

Table 5　2D NMR extraction signals of E_1f^2 shale of Well X1 in Gaoyou Sag

样品编号	抽提前核磁信号强度/au				抽提后核磁信号强度/au			
	类固体有机质	羟基化合物	水	轻质烃	类固体有机质	羟基化合物	水	轻质烃
S-4	0. 393	2. 132	0. 252	0. 259	0. 138	1. 798	0. 123	0. 178
S-5	0. 758	5. 109	0. 119	0. 111	0. 427	4. 736	0. 172	0. 068
S-10	0. 274	2. 677	0. 279	0. 129	0. 209	2. 169	0. 181	0. 071
S-11	0. 675	1. 606	0. 269	0. 329	0. 406	1. 246	0. 192	0. 112
S-20	0. 300	1. 090	0. 476	0. 071	0. 087	1. 215	0. 343	0. 075

表 6　高邮凹陷 X1 井阜二段页岩二维核磁抽提结果

Table 6　2D NMR extraction results of E_1f^2 shale at Well X1 in Gaoyou Sag

样品编号	抽提前含量/(μL/g)					抽提后含量/(μL/g)				
	样品质量/g	类固体有机质	羟基化合物	水	轻质烃	样品质量/g	类固体有机质	羟基化合物	水	轻质烃
S-4	30. 03	2. 62	14. 22	1. 68	1. 73	29. 76	1. 04	13. 49	0. 92	1. 33
S-5	25. 27	7. 00	47. 20	1. 10	1. 02	25. 11	3. 77	41. 81	1. 52	0. 60
S-10	29. 60	2. 04	19. 92	2. 08	0. 96	29. 50	1. 65	17. 13	1. 43	0. 56
S-11	30. 24	3. 69	8. 77	1. 47	1. 80	30. 14	2. 97	9. 13	1. 41	0. 82
S-20	34. 50	2. 61	9. 49	4. 14	0. 62	34. 35	0. 72	9. 95	2. 81	0. 61

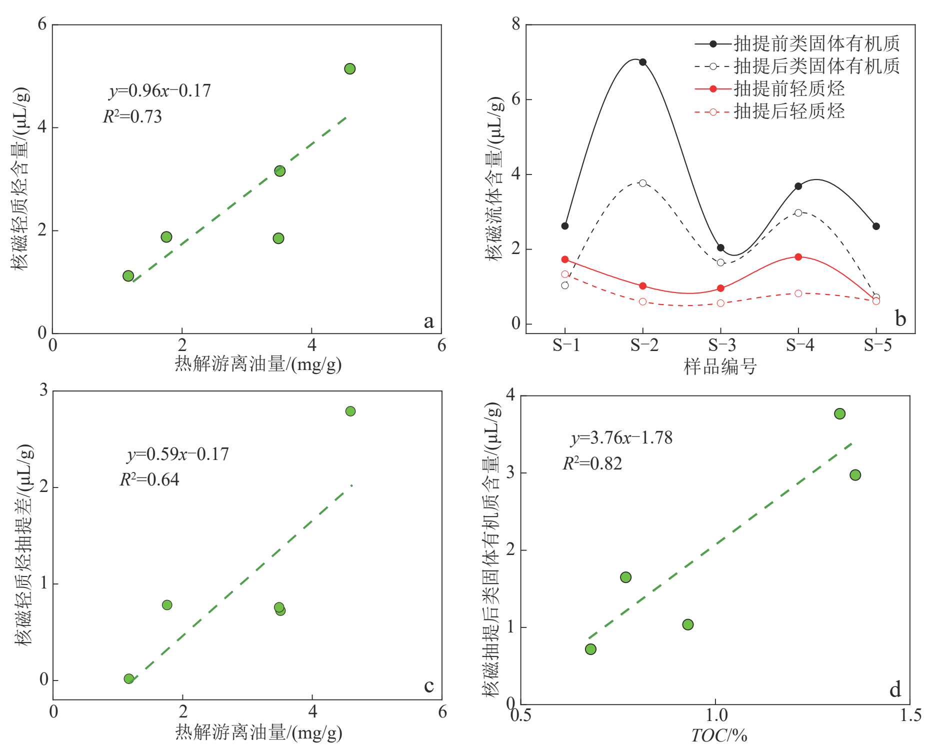

图 8　高邮凹陷 X1 井阜二段页岩二维核磁共振抽提结果分析

Fig. 8　Analysis of 2D NMR extraction results of E_1f^2 shale of Well X1 in Gaoyou Sag

a. 核磁轻质烃含量和热解游离油量关系;b. 核磁轻质烃和类固体有机质抽提结果;c. 核磁轻质烃抽提差和热解游离油量关系;d. 核磁抽提后类固体有机质含量和 *TOC* 关系

质抽提和二维核磁共振实验能直观表现出页岩油不同赋存状态差异性并对其开展定量评价，核磁法得轻质烃与热解游离油量有良好的关系，可以有效表征游离油量。

页1亚段页岩恢复后核磁游离油量3.16 μL/g，热解游离油量平均为3.36 mg/g；页2亚段页岩恢复后核磁游离油量平均1.86 μL/g，热解游离油量平均为3.79 mg/g。二维谱图中游离油、吸附油及自由水区域界限明显，抽提前后各区域信号显示无明显变化。页3亚段页岩恢复后核磁游离油量5.14 μL/g，热解游离油量平均为4.42 mg/g。二维谱图中游离油、吸附油及自由水区域分隔界限明显，抽提后各组分有明显减少，游离油量及其占比高。页5亚段页岩恢复后核磁游离油量1.22 μL/g，热解游离油量为1.17 mg/g，二维谱图游离油和吸附油区域信号显示不明显，吸附烃占比较高（图9）。

4.2 游离油量影响因素

4.2.1 矿物组分

矿物成分影响着储层储集空间类型、发育特征及其物理性质，矿物对烃类物质的吸附能力不同导致烃类流体的非均质分布，影响着页岩游离油的局部富集[35]。随着页岩长英质矿物含量的增加，轻质烃在游离油量中的占比增多、页岩油可动性增强，游离油量先增大后减小。随黏土矿物含量增加，类固体有机质抽提差在总体中占比增多，吸附油量增加（图10）。石英含量增加说明沉积期内陆源碎屑输入量增加，为沉积水体提供大量养分，有利于低等水生生物的生存，提升了古生产力；当长英质含量为40 %时，古生产力达到峰值，陆源碎屑输入量会稀释沉积有机质[36]。黏土质页岩具有高比表面积和较强烃类吸附能力[16]，高黏土

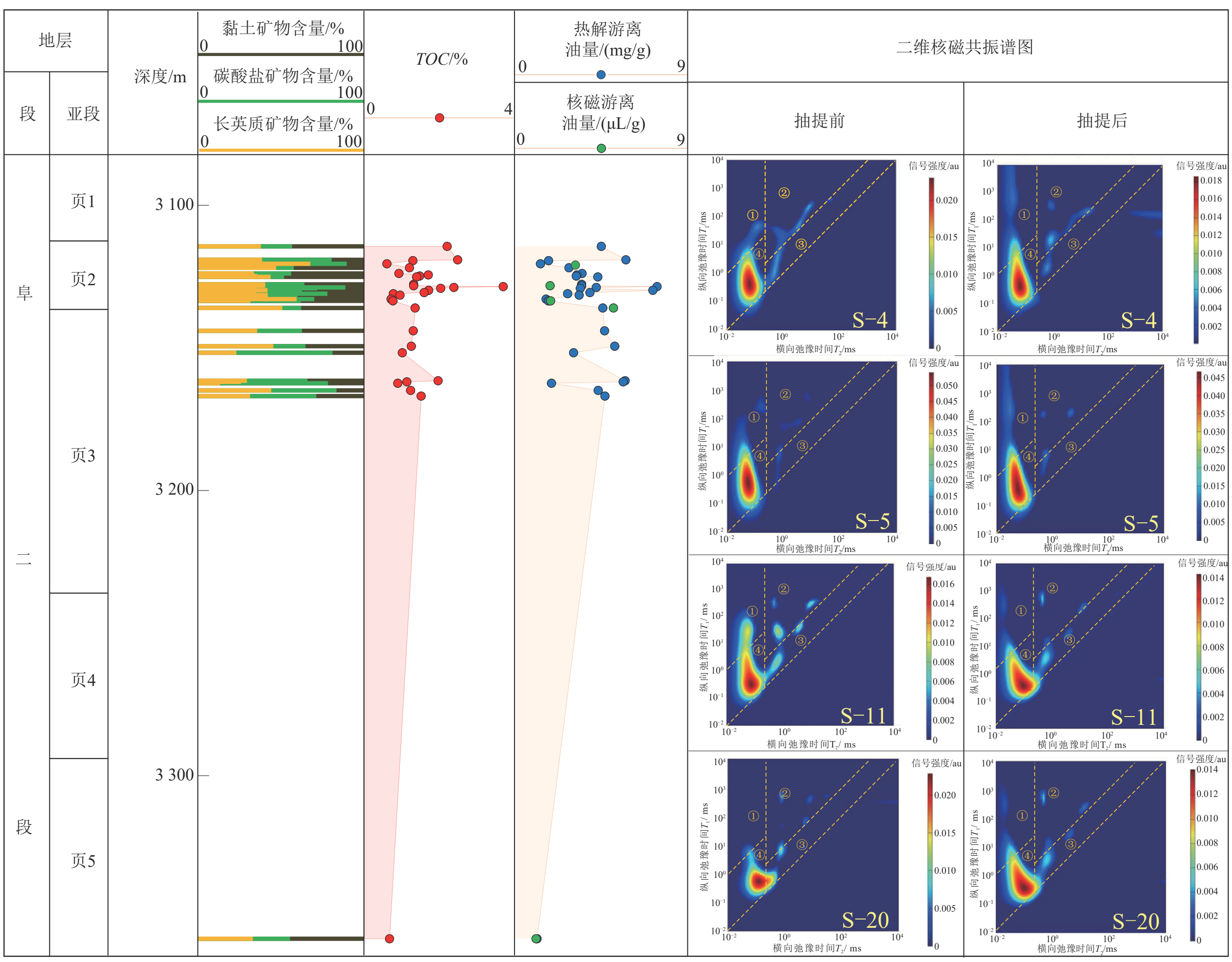

图9　高邮凹陷X1井阜二段页岩游离油量及二维核磁共振谱图

Fig. 9　Free oil content and T_1-T_2 spectra of E_1f^2 shale from Well X1 in Gaoyou Sag

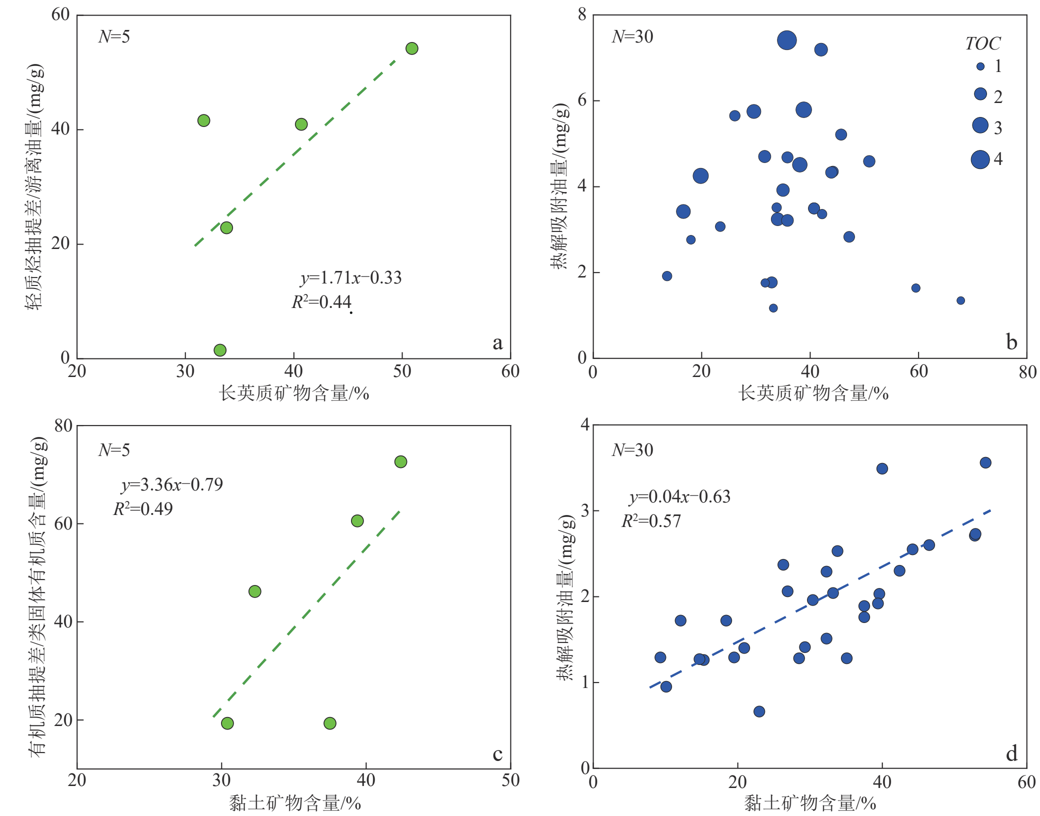

图 10　高邮凹陷 X1 井阜二段页岩矿物含量与游离油量和吸附油量关系

Fig. 10　Correlations between minerals and free, absorbed oil contents of shale from X1 Well of E_1f^2 in Gaoyou Sag

a. 轻质抽提差/游离油量 vs. 长英质矿物含量;b. 热解吸附油量 vs. 长英质矿物含量;c. 有机质抽提差/类固体有机质含量 vs. 黏土矿物含量;d. 热解吸附油量 vs. 黏土矿物含量

矿物含量导致页岩油的吸附位点、吸附油量和吸附比例增多,从而游离油量减少[37]。

4.2.2　有机质

游离油量随着 *TOC* 增加而增加(图 11a)。有机质丰度是烃源岩生烃的物质基础,决定了生烃潜力,当 *TOC* 较低时,干酪根产生的油量无法满足原位吸附/溶胀能力,因而无法向外排出烃类。随着 *TOC* 的增加,页岩油达到原位吸附/膨胀极限,以游离状态滞留在页岩孔隙和裂缝中,游离油量逐渐增加[15]。

Ⅰ型和Ⅱ$_1$型干酪根页岩的游离油量最高(图 11b)。有机质类型与有机母质来源密切相关,不同有机质类型具有不同的生烃潜力。Ⅰ型和Ⅱ$_1$型有机质主要来自藻类、细菌和浮游生物,具有强生油能

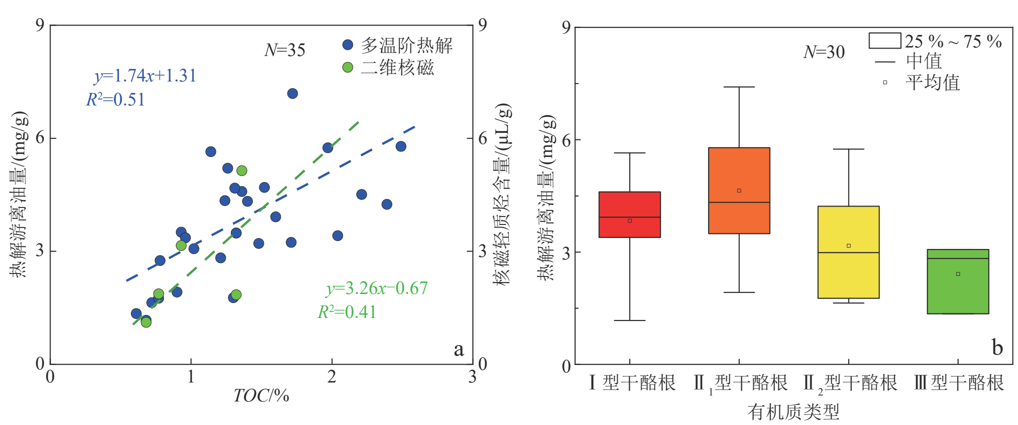

图 11　高邮凹陷 X1 井阜二段页岩 *TOC*(a)和有机质类型(b)与游离油量关系

Fig. 11　Correlations between *TOC*(a), types of organic matter(b) and free oil contents of shale from X1 Well of E_1f^2 in Gaoyou Sag

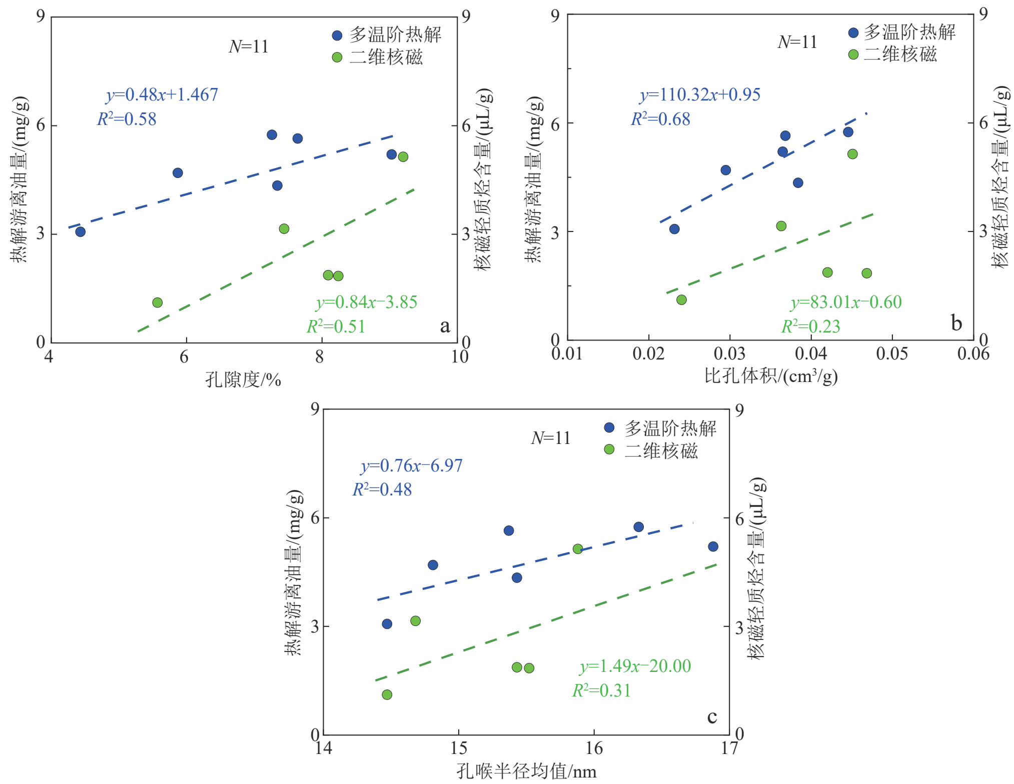

图12 高邮凹陷X1井阜二段页岩孔隙度(a)、比孔体积(b)及孔喉半径均值(c)与游离油量关系

Fig. 12 Correlations between Porosity(a), Specific Pore Volume(b), Median value of pore throat radius (c) and free oil contents of shale from Well X1 of E_1f^2 in Gaoyou Sag

力,在生烃过程中页岩内部超压促进裂缝发育进而加速排油,生成的有机酸使长石等矿物发生溶解作用形成孔隙,为页岩游离油提供赋存空间[38-39]。

4.2.3 储层物性及孔缝结构

页岩储层对页岩游离油量的影响主要在于储集空间、储层物性及孔隙结构,孔隙度、比孔体积、半径均值和游离油量呈正相关关系(图12)。页岩内部烃类通过运移优先占据临近孔隙,且随着成熟度的进一步增加与生烃相关的有机质孔大量形成,页岩中的大量微纳米级无机孔隙和有机孔隙为页岩油的赋存提供了空间[40]。储集空间大小及连通性影响着页岩油的游离及赋存,阜二段页岩储层矿物粒间孔、溶蚀孔等有效孔隙发育,孔隙比孔体积大、连通性好,可以提供有效的游离油储集空间及渗流通道,高孔隙度、高比孔体积、高半径均值有利于游离油流动与富集。

5 结论

1) 高邮凹陷阜二段页岩以混合质页岩为主;*TOC*为0.61 %~3.70 %,烃源岩品质为中-好级别,处于成熟阶段;储集空间主要为晶间孔、粒间孔和有机孔;热解游离油量为1.17~7.41 mg/g。

2) 二维核磁谱图分为轻质油、类固体有机质、羟基化合物和水4个区域,抽提前、后页岩轻质烃含量平均分别为1.23 μL/g和0.79 μL/g,类固体有机质含量平均分别为3.59 μL/g和2.03 μL/g。

3) 二维核磁共振结合有机质抽提实验能定量评价游离油、表征页岩油不同赋存状态差异性,抽提后类固体有机质含量和*TOC*有良好相关关系,抽提前核磁轻质烃含量、核磁轻质烃抽提差都与热解游离油量有较好线性关系。

4) 游离油量随着长英质矿物含量增加呈先增后减趋势,与*TOC*整体上为正相关关系;Ⅰ型和$Ⅱ_1$型干酪根有机质页岩游离油量较其他类型大;适中的成熟度演化使烃类轻组分增多、可动性增强,游离油量增多。只有高孔隙度、高比孔体积及高孔喉半径均值的页岩储层有利于游离油富集。

参 考 文 献

[1] HOU Lianhua, ZOU Caineng, YU Zhichao, et al. Quantitative assessment of the sweet spot in marine shale oil and gas based on geology, engineering, and economics: A case study from the

Eagle Ford Shale, USA[J]. Energy Strategy Reviews, 2021, 38: 100713.

[2] ADEYILOLA A, NORDENG S, ONWUMELU C, et al. Geochemical, petrographic and petrophysical characterization of the Lower Bakken Shale, Divide County, North Dakota[J]. International Journal of Coal Geology, 2020, 224: 103477.

[3] LIU Kouqi, OSTADHASSAN M, GENTZIS T, et al. Characterization of geochemical properties and microstructures of the Bakken Shale in North Dakota[J]. International Journal of Coal Geology, 2018, 190: 84-98.

[4] 李梦莹, 朱如凯, 胡素云. 海外陆相页岩油地质特征与资源潜力[J]. 岩性油气藏, 2022, 34(1): 163-174.
LI Mengying, ZHU Rukai, HU Suyun. Geological characteristics and resource potential of overseas terrestrial shale oil. Lithologic Reservoirs[J], 2022, 34(1): 163-174.

[5] XI Kelai, LI Ke, CAO Yingchang, et al. Laminae combination and shale oil enrichment patterns of Chang 7_3 sub-member organic-rich shales in the Triassic Yanchang Formation, Ordos Basin, NW China[J]. Petroleum Exploration and Development, 2020, 47(6): 1342-1353.

[6] 雷海艳, 郭佩, 孟颖, 等. 玛湖凹陷二叠系风城组页岩油储层孔隙结构及分类评价[J]. 岩性油气藏, 2022, 34(3): 142-153.
LEI Haiyan, GUO Pei, MENG Ying, et al. Pore structure and classification evaluation of shale oil reservoirs of Permian Fengcheng Formation in Mahu Sag[J]. Lithologic Reservoirs, 2022, 34(3): 142-153.

[7] 黎茂稳, 金之钧, 董明哲, 等. 陆相页岩形成演化与页岩油富集机理研究进展[J]. 石油实验地质, 2020, 42(4): 489-505.
LI Maowen, JIN Zhijun, DONG Mingzhe, et al. Advances in the basic study of lacustrine shale evolution and shale oil accumulation[J]. Petroleum Geology & Experiment, 2020, 42(4): 489-505.

[8] 冯动军. 四川盆地侏罗系大安寨段陆相页岩油气地质特征及勘探方向[J]. 石油实验地质, 2022, 44(2): 219-230.
FENG Dongjun. Geological characteristics and exploration direction of continental shale gas in Jurassic Daanzhai Member, Sichuan Basin[J]. Petroleum Geology & Experiment, 2022, 44(2): 219-230.

[9] 崔宝文, 赵莹, 张革, 等. 松辽盆地古龙页岩油地质储量估算方法及其应用[J]. 大庆石油地质与开发, 2022, 41(3): 14-23.
CUI Baowen, ZHAO Ying, ZHANG Ge, et al. Estimation method and application for OOIP of Gulong shale oil in Songliao Basin[J]. Petroleum Geology & Oilfield Development in Daqing, 2022, 41(3): 14-23.

[10] 王永诗, 李政, 王民, 等. 渤海湾盆地济阳坳陷陆相页岩油吸附控制因素[J]. 石油与天然气地质, 2022, 43(3): 489-498.
WANG Yongshi, LI Zheng, WANG Min, et al. Factors controlling lacustrine shale oil adsorption in the Jiyang Depression, Bohai Bay Basin[J]. Oil & Gas Geology, 2022, 43(3): 489-498.

[11] JIN Zhijun, LIANG Xinping, BAI Zhenrui. Exploration breakthrough and its significance of Gulong lacustrine shale oil in the Songliao Basin, Northeastern China[J]. Energy Geoscience, 2022, 3(2): 120-125.

[12] 沈云琦, 金之钧, 苏建政, 等. 中国陆相页岩油储层水平渗透率与垂直渗透率特征——以渤海湾盆地济阳坳陷和江汉盆地潜江凹陷为例[J]. 石油与天然气地质, 2022, 43(2): 378-389.
SHEN Yunqi, JIN Zhijun, SU Jianzheng, et al. Characteristics of horizontal and vertical permeability of continental shale oil reservoirs in China: A case from Jiyang Depression in Bohai Bay Basin and Qianjiang Sag in Jianghan Baisn[J]. Oil & Gas Geology, 2022, 43(2): 378-389.

[13] 黎茂稳, 马晓潇, 金之钧, 等. 中国海、陆相页岩层系岩相组合多样性与非常规油气勘探意义[J]. 石油与天然气地质, 2022, 43(1): 1-25.
LI Maowen, MA Xiaoxiao, JIN Zhijun, et al. Diversity in the lithofacies assemblages of marine and lacustrine shale strata and significance for unconventional petroleum exploration in China[J]. Oil & Gas Geology, 2022, 43(1): 1-25.

[14] CAO Zhe, JIANG Hang, ZENG Jianhui, et al. Nanoscale liquid hydrocarbon adsorption on clay minerals: A molecular dynamics simulation of shale oils[J]. Chemical Engineering Journal, 2021, 420(Part 3): 127578.

[15] HU Tao, PANG Xiongqi, JIANG Fujie, et al. Movable oil content evaluation of lacustrine organic-rich shales: Methods and a novel quantitative evaluation model[J]. Earth-Science Reviews, 2021, 214: 103545.

[16] 蒋启贵, 黎茂稳, 马媛媛, 等. 页岩油可动性分子地球化学评价方法——以济阳坳陷页岩油为例[J]. 石油实验地质, 2018, 40(6): 849-854.
JIANG Qigui, LI Maowen, MA Yuanyuan, et al. Molecular geochemical evaluation of shale oil mobility: A case study of shale oil in Jiyang Depression[J]. Petroleum Geology and Experiment, 2018, 40(6): 849-854.

[17] LI Chaoliu, YAN Weilin, WU Hongliang, et al. Calculation of oil saturation in clay-rich shale reservoirs: A case study of Qing 1 Member of Cretaceous Qingshankou Formation in Gulong Sag, Songliao Basin, NE China[J]. Petroleum Exploration and Development, 2022, 49(6): 1351-1363.

[18] 钱门辉, 蒋启贵, 黎茂稳, 等. 泥页岩三维定量荧光分析技术与应用[J]. 石油实验地质, 2020, 42(2): 311-318.
QIAN Menhui, JIANG Qigui, LI Maowen, et al. Three-dimensional quantitative fluorescence analysis and application in shale[J]. Petroleum Geology and Experiment, 2020, 42(2): 311-318.

[19] LIU Bo, BAI Longhui, CHI Yaao, et al. Geochemical characterization and quantitative evaluation of shale oil reservoir by two-dimensional nuclear magnetic resonance and quantitative grain fluorescence on extract: A case study from the Qingshankou Formation in Southern Songliao Basin, northeast China[J]. Marine and Petroleum Geology, 2019, 109: 561-573.

[20] XU Yi, LUN Zengmin, PAN Zhejun, et al. Occurrence space and state of shale oil: A review[J]. Journal of Petroleum Science and Engineering, 2022, 211: 110183.

[21] XU Chenyu, XIE Ranhong, GUO Jiangfeng, et al. Comprehensive characterization of petrophysical properties in shale by solvent extraction experiments and 2D NMR[J]. Fuel, 2023, 335: 127070.

[22] SONG Yiqiao, KAUSIK R. NMR application in unconventional shale reservoirs-A new porous media research frontier[J]. Progress in Nuclear Magnetic Resonance Spectroscopy, 2019, 112/113: 17-33.

[23] ZHU Chaofan, GUO Wei, LI Yajun, et al. Effect of occurrence states of fluid and pore structures on shale oil movability[J].

Fuel, 2021, 288: 119847.

[24] SUI Hongguang, ZHANG Fenyun, WANG Ziqiang, et al. Molecular simulations of oil adsorption and transport behavior in inorganic shale[J]. Journal of Molecular Liquids, 2020, 305: 112745.

[25] WANG Sen, JAVADPOUR F, FENG Qihong. Molecular dynamics simulations of oil transport through inorganic nanopores in shale [J]. Fuel, 2016, 171: 74-86.

[26] HUANG Hexin, LI Rongxi, CHEN Weitao, et al. Revisiting movable fluid space in tight fine-grained reservoirs: A case study from Shahejie shale in the Bohai Bay Basin, NE China[J]. Journal of Petroleum Science and Engineering, 2021, 207: 109170.

[27] MENG Ziyuan, SUN Wei, LIU Yiqun, et al. Effect of pore networks on the properties of movable fluids in tight sandstones from the perspective of multi-techniques[J]. Journal of Petroleum Science and Engineering, 2021, 201: 108449.

[28] GAO Gang, YANG Shangru, ZHANG Weiwei, et al. Organic geochemistry of the lacustrine shales from the Cretaceous Taizhou Formation in the Gaoyou Sag, Northern Jiangsu Basin[J]. Marine and Petroleum Geology, 2018, 89(Part 3): 594-603.

[29] 付茜, 刘启东, 刘世丽, 等. 苏北盆地高邮凹陷古近系阜宁组二段页岩油成藏条件分析[J]. 石油实验地质, 2020, 42(4): 625-631.

FU Qian, LIU Qidong, LIU Shili, et al. Shale oil accumulation conditions in the second member of Paleogene Funing Formation, Gaoyou Sag, Subei Basin[J]. Petroleum Geology and Experiment, 2020, 42(4): 625-631.

[30] 钱门辉, 黎茂稳, 蒋启贵, 等. 页岩岩心样品烃类散失特征与地质意义[J]. 石油实验地质, 2022, 44(3): 497-504, 514.

QIAN Menhui, LI Maowen, JIANG Qigui, et al. Evaluation of evaporative loss of hydrocarbon in shale samples and its geological implications[J]. Petroleum Geology and Experiment, 2022, 44(3): 497-504, 514.

[31] 赵贤正, 金凤鸣, 周立宏, 等. 渤海湾盆地风险探井歧页1H井沙河街组一段页岩油勘探突破及其意义[J]. 石油学报, 2022, 43(10): 1369-1382.

ZHAO Xianzheng, JIN Fengming, ZHOU Lihong, et al. Breakthrough and significance of shale oil exploration in Member 1 of Shahejie Formation of Well Qiye 1H, a risk exploratory well in Bohai Bay Basin[J]. Acta Petrolei Sinica, 2022, 43(10): 1369-1382.

[32] 中国石油天然气总公司. 陆相烃源岩地球化学评价方法: SY/T 5735-1995[S]. 北京: 石油工业出版社, 1996.

China National Petroleum Corporation. Geochemical evaluation method of continental source rock: SY/T 5735-1995[S]. Beijing: Petroleum Industry Press, 1996.

[33] LI Jinbu, JIANG Chunqing, WANG Min, et al. Adsorbed and free hydrocarbons in unconventional shale reservoir: A new insight from NMR T_1-T_2 maps[J]. Marine and Petroleum Geology, 2020, 116: 104311.

[34] MA Xiao, GUO Shaobin, SHI Dishi, et al. Investigation of pore structure and fractal characteristics of marine-continental transitional shales from Longtan Formation using MICP, gas adsorption, and NMR (Guizhou, China)[J]. Marine and Petroleum Geology, 2019, 107: 555-571.

[35] WANG Xin, WANG Min, LI Jinbu, et al. Thermal maturity: The controlling factor of wettability, pore structure, and oil content in the lacustrine Qingshankou shale, Songliao Basin[J]. Journal of Petroleum Science and Engineering, 2022, 215(Part A): 110618.

[36] DONG Tian, WANG Chuan, LIANG Xing, et al. Paleodepositional conditions and organic matter accumulation mechanisms in the Upper Ordovician-Lower Silurian Wufeng-Longmaxi shales, Middle Yangtze region, South China[J]. Marine and Petroleum Geology, 2022, 143: 105823.

[37] HOU Lianhua, WU Songtao, JING Zhenhua, et al. Effects of types and content of clay minerals on reservoir effectiveness for lacustrine organic matter rich shale[J]. Fuel, 2022, 327: 125043.

[38] YANG Meihua, ZUO Yinhui, YAN Kangnan, et al. Hydrocarbon generation history constrained by thermal history and hydrocarbon generation kinetics: A case study of the Dongpu Depression, Bohai Bay Basin, China[J]. Petroleum Science, 2022, 19(2): 472-485.

[39] LIANG Tian, ZHAN Zhaowen, ZOU Yanrong, et al. Research on type I kerogen molecular simulation and docking between kerogen and saturated hydrocarbon molecule during oil generation[J]. Chemical Geology, 2023, 617: 121263.

[40] 徐学敏, 杨佳佳, 孙玮琳, 等. 页岩油气勘探中热解分析与总有机碳预测[J]. 中国石油大学学报(自然科学版), 2022, 46(4): 22-29.

XU Xuemin, YANG Jiajia, SUN Weilin, et al. Pyrolysis analysis and total organic carbon prediction in shale oil and gas exploration [J]. Journal of China University of Petroleum(Edition of Natural Science), 2022, 46(4): 22-29.

[41] SU Siyuan, JIANG Zhenxue, SHAN Xuanlong, et al. The effects of shale pore structure and mineral components on shale oil accumulation in the Zhanhua Sag, Jiyang Depression, Bohai Bay Basin, China[J]. Journal of Petroleum Science and Engineering, 2018, 165: 365-374.

[42] 冷筠滢, 钱门辉, 鹿坤, 等. 渤海湾盆地东濮凹陷北部页岩油富集类型和烃类组成特征——以文410井古近系沙河街组三段为例[J]. 石油实验地质, 2022, 44(6): 1028-1036.

LENG Junying, QIAN Menhui, LU Kun, et al. Enrichment types and hydrocarbon composition characteristics of shale oil in the northern part of Dongpu Sag, Bohai Bay Basin: a case study of the third member of Paleogene Shahejie Formation of well Wen 410 [J]. Petroleum Geology & Experiment, 2022, 44(6): 1028-1036.

[43] 文志刚, 罗雨舒, 刘江艳, 等. 陇东地区三叠系长7段页岩油储层孔隙结构特征及成因机制[J]. 岩性油气藏, 2022, 34(6): 47-59.

WEN Zhigang, LUO Yushu, LIU Jiangyan, et al. Pore structure characteristics and genetic mechanism of Triassic Chang 7 shale oil reservoir in Longdong area[J]. Lithologic Reservoirs, 2022, 34(6): 47-59.

(编辑 张亚雄)